Webology (ISSN: 1735-188X)
Volume 19, Number 3, 2022

A Review On Application Of Deep Learning For Lung Infection Detection On Different Medical Images

Shaba Parveen Khan[1] , Dr. Manu Banga[2]

[1]Amity University Rajasthan, Jaipur. ORCID iD:0000-0001-5718-6211

[2]Amity University Rajasthan, Jaipur.

Abstract

Infectious diseases in the respiratory system are a significant source of death and disability across the world. Despite the fact that radiology is the main diagnostic technique for monitoring lung related infections, visual analysis of MRI's and computerized tomography (CT) scans is confined due to low quality for causational potential pathogens and a restricted ability to evaluate severity and anticipate health outcomes. Herein, in this paper a review on the imaging characteristics and computing models that have been applied for the management of COVID-19 are presented such as CT positron emission tomography-CT (PET/CT), magnetic resonance imaging (MRI), Fluorodeoxyglucose (FDG)-positron emission tomography (PET) have been used for detection, treatment, and follow-up. Also, highlight the limitations of identifying and characterizing these illnesses using Medical Imaging with deep learning, and provide potential solutions to these problems. Thus, this paper gives special attention to the role of Deep learning and various Medical Imaging techniques in the diagnosis and therapy monitoring of infectious and inflammatory diseases. Enough evidence in the literature already exists about the usefulness of FDG-PET/CT in the diagnosis and management of patients.

Keywords: Lung Infection, COVID-19, CT, MRI, FDG-PET, Deep Learning.

1. Introduction

A respiratory infection may vary in severity from minor to deadly. Even though the majority of respiratory infections are curable and yet most patients recovered, they can also quite hazardous. This one is particularly true for newborns, the elderly, as well as those suffering from lung illness or a compromised immunity [1]. Pneumonia is a pulmonary pathogen that affects inflammation and swelling Trusted Source. One of the most frequent lung illnesses is tuberculosis. Pneumonia can be caused by bacterial, fungus, or viruses. Tuberculosis (TB), it is caused by infectious bacteria called Mycobacterium tuberculosis. The sooner a patient receives treatments for tuberculosis, less probable individuals will be to infect humans or suffer major side effects. Influenza is an illness of the organs that are involved in breathing that affecting both the whole upper as well as lower respiratory tracts, including that of nose with neck. Bronchitis, this is a disease of bronchial tubes, that aid as in inhalation of Oxygen (O_2) by the breath. The illness, like pneumonia, could be bacterial or viral. Bordetella pertussis is the bacterium that causes pertussis. Such lung disease is

characterized by continuous, severe coughs which can cause breathing difficult. Lung cancer, from the other side, is caused by uncontrolled cell growth that results in tumors. A lung nodule is a lung anomaly defined by a tiny circular shape or elliptic tumor inside the lung usually emerges like a white shadow on a Computed tomography and can develop to lung cancer. Radiographers can benefit from a computer-aided lung nodule identification structure that enables them discover lung abnormalities earlier [1].

Covid-19, the SARS-CoV-2 virus causes Corona Virus illness, which is an infection in the Respiratory Organs. Significantly bigger pulmonary droplets to tiny aerosols are among the particles. In certain circumstances, it is extremely harmful, with an estimated 4.9 million fatalities. Many technological studies have been conducted to address issue, including the use of image processing methods such as deep learning networks (DNN) to diagnose COVID19 primarily on X-Ray images [2].

Respiratory infections can be diagnosed using a variety of methods, including chest radiography (x-ray), Highly advanced computed tomography (CT), magnetic resonance (MRI scan), as well as sputum cytology. [2] To study the Respiratory system illnesses inside the body, the Computer Aided Diagnosis (CAD) systems involve preprocessing including feature extraction using X-rays, as well as a Computer Tomography (CT) scan [3]. In the realm of visual interpretation, highly advanced Artificial Intelligence (AI) using Machine Learning, especially Deep Learning, has led to important breakthroughs in recognizing, classifying, as well as quantifying patterns in diagnostic images [4]. When determined by the standard machine learning (ML) approaches, deep learning (DL) models have acquired a lot of traction. Unlike ML approaches, DL method performed all steps of extracting features, image segmentation, and classifications automatically. In difficulties concerning medical scanning, digitally aided image processing has become critical. By using machine learning approaches, here to the input datasets, it is necessary to preprocess as well as analyze medical field datasets including X-Rays films, scan by Computed Tomography (CT) images [5]. Because of its adaptability in building improved models and detecting abnormalities in various CT scans or X-ray images, the image processing approach is the most preferred. Fig 1 depicts the flow of processes to be completed in procedures. On CT Scan or X-ray images, follow the given steps: image acquisition, image enhancements, tumor categorizations, feature extraction, image segmentations, etc.

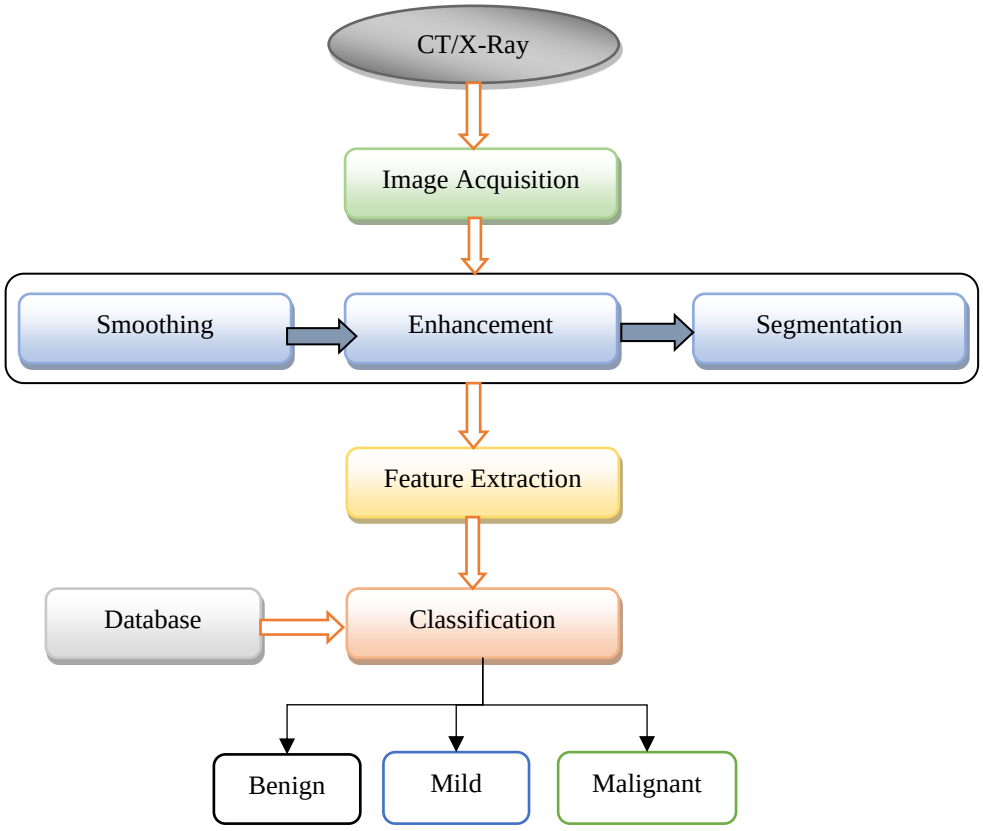

Fig 1. The steps of Image Processing Technique for Lung Disease Diagnosis (LDD)

If it comes to knowing representations datasets, deep learning (DL) is a type of advanced machine learning (ML) which uses numerous computational steps to obtain a high level of information. Most image segmentation methodologies have been superseded by Convolutional Neural Network (CNN) that is a subset of ML and a subclass of DL (Deep Learning methods that used semantic segmentation). For depict greater level but also sophisticated datasets abstraction, it uses multiple layer processing. CNNs have gained popularity as a result of their increased image categorization effectiveness. The architectures Convolutional layers, as well as the filters, aid in retrieving temporal and spatial characteristics from images.

2. Application of Image Processing for COVID-19 Detection

Abdulmunem et al. [2] proposed a technique for classifying COVID19 relying on x-ray images that uses deep learning networks. The findings are promising and may be used to distinguish infected individuals from healthy ones. To deal with the issue, the author employs substantial machine learning techniques (Deep learning networks), which have shown to be effective in the medical sector. ResNet50 is the deep network which utilize. On the Kaggle website, tested the deep network on the latest COVID19 dataset. Deep learning produces solid results in classifying covid infected individuals based on their x-ray images, with a recognition rate of 97.28 percent in 5-fold cross-validation tests and 95.99 percent in 10-fold cross-validation tests. The recognition rate in 5-folds is greater than the recognition rate in 10-folds, as indicated.

Rahimzadeh et al. [6] proposed completely automated method for COVID-19 identification from lung HRCT images. Author released a fresh dataset comprising 15,589 images of healthy people and 48,260

photographs of COVID-19 patients. Initially, presented an image processing method for filtering the correct images of the patients' CT scans, which precisely depict the interior of the lung. This method aids in the improvement of network accuracy as well as speed. 3 distinct deep convolutional networks trained to identify CT scan images as COVID-19 or normal. The best results were obtained by model, which included ResNet50V2, the modified feature pyramid system network with proposed architecture. Tested in 2 ways, first 7796 images second 245 patients with 41,892 photographs different thicknesses. This has an overall accuracy of 98.49% for single image categorization (I assessment method). For patient situation identification stage (II assessment method), model accurately identifying 234 out of 245 patients. Utilized the Grad-CAM algorithm to evaluate the classification accuracy and highlight the infection spots in CT scan images. Based on the findings, it's clear that now the suggested techniques can enhance COVID-19 detection while also being quick enough to be used in medical settings.

Hassantabar et al. [7] utilized 3 deep learning-based techniques in this work to identify and diagnose COVID-19 patients using X-Ray images of the lungs. Proposed two algorithms for illness diagnosis: a deep neural network (DNN) on the fractal feature of images and a convolutional neural network (CNN) approach that uses lung images directly. The proposed CNN architecture, with a greater accuracy (93.2%) and sensitivity (96.1%), outperforms the DNN approach, which has an accuracy of 83.4 percent and a sensitivity of 86 percent, then used a CNN architecture to identify infectious tissue in lung images during the segmentation phase. The proposed technique can virtually identify contaminated areas with a high accuracy of 83.84 percent, according to the results. This discovery may potentially be utilized to monitor and manage contaminated area expansion in patients. Reverse Transcription Polymerase Chain Reaction is now the important technique for diagnosing patients (RT-PCR), But costly and time consuming. The resulting technique may be used in place of RT-PCR.

Wang et al. [8] presented COVID-Net, an open source and publicly accessible deep convolutional neural network architecture optimized for the identification of COVID-19 cases using chest X-ray (CXR) images. COVID-Net is also one of the earliest open source network architectures for COVID-19 detection using CXR images, when it was initially released. COVIDx, an open-access benchmark dataset made up of 13,975 CXR images from 13,870 patient cases, with the highest amount of publicly accessible COVID-19 positive patients. Proposed process of generating the COVIDx dataset, the architectural design technique underlying the suggested COVID-Net, the resultant network architecture, implementation details in constructing COVID-Net, and the approach for auditing COVID-Net. To have a better grasp of its detection accuracy, do both quantitative as well as qualitative study. COVID-Net demonstrates excellent accuracy by attaining 93.3 percent test accuracy, demonstrating the effectiveness of using a human-machine collaborative approach for rapidly building highly-customized CNN architectures suited to task, data, and system requirements.

Sakshi et al. [9] conducted a three-phase technique for classifying the COVID-19 and non-COVID-19 lung CT scan slices. Phase one, data augmentation is used to divide CT scan slices into three levels applying stationary wavelets. Expand the dataset size, like random rotation with translation, as well as shear. In phase 2, 4 distinct transfer learning-based architecture, ResNet18 and ResNet50 and two other ResNet101, and SqueezeNet, are used to conduct a two-level classification, and results validated. The ResNet18 uses the transfer learning model to obtain the best classification accuracy both training (99.82%) as well as validation (97.32%). The testing results show that the accuracy is 99.4 percent, the sensitivity is 100 percent, the specificity is 98.6 percent, and the AUC is 0.9965. In phase 3, the best performing model (ResNet18) was chosen and applied for abnormality localisation in COVID-19 positive patients' chest CT scan sections.

The proposed model will undoubtedly aid in the fast and precise identification of COVID-19 signatures from CT scan sections of the lungs.

Ozturk et al. [10] developed a deep learning-based approach to identify also classify COVID-19 instances from X-ray images in this research. COVID-19 were detected using deep learning model named Dark Covid Net in this research. To build model, Utilized 1125 images (125 COVID-19(+), 500 Pneumonia, and 500 No-Findings). This system has an end-to-end structure that eliminates necessity manual feature extraction. The accuracy of created system in binary as well as multi-class tasks is 98.08 percent and 87.02 percent, respectively. Other chest-related illnesses, such as TB and pneumonia, may also be diagnosed using similar models. X-ray radiographs may be utilized to diagnose COVID-19 using the suggested paradigm. Because X-ray radiographs are easily available for illness diagnosis, they are recommended. The model can diagnose COVID-19 in a matter of seconds. The study's utilization of a restricted numbers COVID-19 X-ray images is a drawback

Chen et al. [11] provided an automated technique for segmenting pulmonary parenchyma in chest Computed tomography and analyzing textural characteristics out from segmented pulmonary parenchyma sections to help radiologists diagnose COVID-19. To segment pulmonary parenchyma in lung Computed tomography scan, a novel segmentation technique was suggested that combines a 3-dimensional (3D) V-Net with such a shape deformation module built that used a spatial transform network (STN). Manual annotation produced by experienced operator was used to verify the suggested segmentation technique. To detect COVID-19 infection, advanced statistical models used to evaluate the radiomic features using our segmentation. The suggested segmentation technique obtained the Dice similarity coefficient 0.9796, sensitivity 98.40%, specificity 99.54%, as well as a mean surface distance error equal 0.0318 mm when compared to the standard annotation. Additionally, utilizing statistically significant radiomic characteristics, an auc value (AUC) 94.70%, sensitivity 96.70%, and then specificity 92.70% when distinguishing COVID-19 lung infection by community-acquired pneumonia and healthy controls.

Oluwasanmi et al. [12] investigated the application of deep learning as well as convolutional neural networks for extracting the features from images and supervised image categorization into predefined groups. Therefore, in machine learning, we use the idea of transfer learning to decrease both times with also computational complexity while still achieving great results. Testing this by putting five pretrained convolutional designs to the test, all of which provide better classification accuracies. Due to the scarcity of COVID-19 data, look at the potential of semi supervised learning, which involves using vast amounts of unlabeled data to improve a model's capacity to recognize features but also patterns in data. Building a semi supervised classifier with 2 types of discriminators both to labelled and unlabeled data using the extremely successful generative adversarial instructional methods, delivering state-of-the-art categorization with little labeled training data. With just a accuracy rate of 94%, sensitivity of 96%, as well as specificity of 92%, this semi supervised model appears to be a highly effective diagnostic tool in COVID-19 classification.

Ohata et al. [13] presented an automated COVID-19 infection detection technique relying on chest X-ray images under this paper. 194 X-ray images of diagnosed cases with coronavirus with 194 X-ray scans of healthy individuals were used to create the datasets for this research. Using the idea of transfer learning with this assignment since there are limited images of patients with COVID-19 that are publicly accessible. Adapt various architectures of ImageNet-trained convolutional neural networks (CNNs) to function as feature extraction for X-ray images. The CNNs are then integrated with machine learning techniques like k-Nearest Neighbor, Bayesian, Random Forest, multilayer perceptron (MLP), as well as support vector machine (SVM). The findings indicate that the Mobile Net architecture also with SVM classifier employing a linear kernel, which obtains an accuracy and also F1-score of 98.5 percent, is the extractor-classifier

combined with the greatest performance for the one of the datasets. DenseNet201 with MLP is the best combination for the other datasets, accuracy with F1-score of 95.6 percent. As a result, the suggested method is effective in detecting COVID19 through X-ray images.

Rajinikanth et al. [14] extracted and analyzed the Coronavirus infection (COVID-19) induced pneumonia infection in the lungs. To extract COVID-19 affected regions from lung CT images, we present an image-assisted method (coronal view). The steps are as follows: i. Image enhancement utilizing Harmony-Search-Optimization with Otsu thresholding; (ii) Image segmentation to recover affected region(s); with (iii) Region-of-interest (ROI) extraction (feature) by binary image to calculate degree of severity. The characteristics recovered from ROI used to calculate the pixel ratio here between lung with infection regions in order to determine the severity of the virus. The tool's main goal is to aid the pulmonologist in not only detecting but also planning the treatment procedure. As a result, it will aid in the reduction of diagnostic load in mass screening processes.

Kunwei et al.[15] performed in Zhuhai, China, a retrospective single-center research on COVID-19 patients from 18 Jan -7 Feb , 2020. Patients being classified into three categories: mild (little symptoms, negative CT results), common, then severe-critical (patients with positive CT). All acute lung inflammatory lesions affecting 5 lobe on the CT visual quantitative assessment. The 5 lobe ratings were added together to get total severity score (TSS). Two observers' consistency was assessed. The clinical categorization was matched to the TSS. The ability of TSS to diagnose severe-critical type was tested using ROC. The CT visual quantitative study has a high level of consistency and can accurately represent the COVID-19 clinical categorization. There were 78 individuals, 38 men and 40 women. The area under the curve (AUC) of TSS for detecting severe-critical type was 0.918, according to ROC analysis. The TSS threshold of 7.5 exhibited a sensitivity of 82.6 percent and a specificity of 100 percent. The CT visual quantitative assessment shows good level of consistency. The severe critical type category had a substantially higher median TSS than for the common type group.

Hemdan et al. [16] presented a novel deep learning framework, COVIDX-Net, to help radiologists detect COVID-19 in X-ray images automatically. The research is verified using 50 chest X-ray images with 25 reported positive COVID-19 patients. The COVIDX-Net contains seven alternative deep CNN designs, including the updated VGG19 and Google Mobile Net's second edition. Each deep CNN model can identify negative or positive COVID-19 case by analyzing the normalized intensity of the X-ray image. The COVIDX-Net has been satisfactorily tested and evaluated using 80-20 percent of X-ray images for the model training stage, With f1-scores of 0.89 as well as 0.91 for regular and COVID-19, respectively. The InceptionV3 model had the lowest accuracy of all the classifiers evaluated, at 50%, VGG19 as well as DenseNet201 had highest accuracy (90 percent). Despite the fact that the MobileNetV2 model has a reasonable aroung 60 percent. The InceptionV3 model had the poorest classification efficiency, f1-scores of 0.67 for common and 0.00 on COVID-19 cases. Based on the suggested COVIDX-Net architecture, this research showed the usefulness of using deep learning models for categorizing COVID-19 in X-ray images.

Fan et al. [17] presented Inf-Net, a new COVID-19 lung CT infection segmentation network that uses implicit reverse attention with explicit edge-attention to enhance infected area detection. Developed Semi-Inf Net a semi-supervised approach to address the scarcity of high-quality data sets. Extensive testing COVID-Semi Seg datasets as well as actual CT volumes has shown that the suggested Inf-Net and Semi-Inf-Net segmentation models excel cutting-edge segmentation methods and enhance state-of-the-art efficiency. This method does have a lot of promise for evaluating COVID-19 diagnosis, such as measuring infected areas, tracking longitudinal illness changes, as well as mass screening processing. Method can

distinguish between infections and normal tissues by detecting items with low intensity contrast. This is a common occurrence in natural camouflage items.

Rahman et al. [18]used digital x-ray images to identify bacterial or viral pneumonia automatically. It starts with a comprehensive report on improvements in accurate pneumonia diagnosis. For transfer learning, 4 distinct deep Convolutional Neural Networks (CNNs): Alex Net and ResNet18 and two other DenseNet201, and Squeeze Net. 5247 chest X-ray images had been preprocessed then trained for such transfer learning-based classification problem, which included bacterial, viral, as well as normal chest X-ray images. The authors provide 3 categorization systems in this study: normal against pneumonia, bacterial versus viral pneumonia then normal-bacterial-viral pneumonia. Normal-pneumonia images, bacterial-viral pneumonia images, and normal-bacterial-viral pneumonia images had classification accuracy of 98 percent, 95 percent, and 93.3 percent, respectively. This is the greatest accuracy among the accuracies recorded in the literature. As a result, the suggested research may aid in the faster diagnosis of pneumonia by radiologists and the screening of pneumonia patients.

Roy et al. [19] used a combination of biomedical image processing techniques with knowledge discovery in datasets to develop precision and establish specific value for early diagnosis of lung cancer. The image of the lungs acquired by CT(Computed Tomography) scan is pre-processed, and segmentation within ROI is performed, with the Random Forest technique used to categorize the unique characteristics. Saliency Enhancement was performed, and characteristics such as entropy, co-relation, energy, and variance were retrieved from the Saliency Enhanced images using the SURF (Speeded Up Robust Features) method and an SVM (The Support Vector Machine) Classifiers. The image's classification determines whether this is healthy or harmful (carcinomic). The method's performance is evaluated using a minimum goal vs. number of functions evaluation plot. The random forest method and SVM classification were used to carry out the whole procedure. Using SVM classification, the best result is achieved. This technique is 94.5 percent efficient in total, 74.2 percent sensitive, 66.3 percent recall, and 77.6% specific.

Li et al. [20] Corona Virus detection neural network (COV Net), a deep learning model, was built to extract visual characteristics from volumetric chest CT scans for the detection of COVID-19 in this research. The model's robustness was tested by including community-acquired pneumonia (CAP) as well as other non-pneumonia CT examinations. The area under receiver operating (AUC), sensitivity, and specificity were used to evaluate diagnostic performance. A total of 4356 computed Tomographic examinations from 3,322 individuals were included in the study. COV Net can extract 2D local as well as three dimensional global representative characteristics. The basis of the COV Net architecture is a RestNet50. In identifying COVID-19, this model has a high sensitivity (90 percent [95 percent CI: 83 percent, 94 percent]) and a high specificity (96 percent [95 percent CI: 93 percent, 98 percent]. COVID-19 and community-acquired pneumonia (CAP) had AUC values of 0.96 [95 percent confidence interval: 0.94, 0.99] and 0.95 [95 percent confidence interval: 0.93, 0.97], respectively.

Oulefki et al. [21] developed and test an automated method for Corona Virus, Lung Infection segmentation as well as quantification utilizing chest CT scans. In comparison to state-of-the-art segmentation methods such as Graph Cut the other Medical Image Segmentation (MIS), the Watershed, comprehensive computer simulations indicate that our end-to-end learning method on Computed tomography image segmentation using image enhancement is more efficient and flexible. In method Kapurs Entropy, Combining linear with logarithmic stitching parametric methods to create a novel image contrast enhancement technique. Experiments were conducted using the COVID-CT-Dataset, which included (275) positive COVID-19 CT scans as well as fresh data out from EL-BAYANE Center of Radiology-Medical Imaging. The accuracy 98%, sensitivity 73%, F-measure 71%, precision 71%, MCC 71%, Dice 57%, Jacquard, and specificity

mean values are 99%, which is better than the techniques described above. The obtained findings demonstrate that the suggested method is more reliable, accurate, and simple.

Elbakary et al. [22] provided a computational visual analysis approach for infections identification in CT scans that utilizes a limited number of COVID-19 CT images. The suggested approach creates a lung mask by using an effective segmentation algorithm with morphological procedures to separate the lung region after eliminating isolated high intensity areas out from surrounding ribs inside the input CT image. This segmented lung mask is then used in the suggested methodology to identify regions of infections inside the lungs. To differentiate between illness versus non-disease sections inside the lung, a variance of the each section's gray-level is calculated and utilized as a feature to identify disease regions with low variance as compared to non-COVID-19 sections. On such a datasets of 72 Computed tomography (36 Non-Covid-19 images , 36 Covid-19 scans) with ground-truth produced by radiologists, the performance of the proposed approach is assessed. Covid-19 image detection accuracy is 91.7 percent, whereas Non-Covid-19 image detection accuracy is 91.7 percent. The suggested method is unable to differentiate between COVID-19 illness and other lung disorders in patients.

Kalaivani et al. [23] identified lung cancer nodules using image preprocessing and segmentation. These procedures are used to identify nodules to obtain characteristics then utilized to categorize the illness stages. Utilizing image processing methods, for detecting lung cancer. Compared to X-ray and MRI images, these images have less noise. The time element is taken into consideration. The images obtained by the CT scanner are processed. From the original image, the area of interest, i.e. the tumor, is correctly recognized. For the pre-processing stage, the Gabor filter with watershed segmentation provide the best results. 3 characteristics are retrieved from the extracted region of interest: area, perimeter, and eccentricity. These 3 characteristics aid in determining the stage of lung cancer. The suggested technique may correctly identify the stage of lung cancer by measuring the tumor's size. Support Vector Machines are also an appealing method to data modeling for classification purposes. They combine generalization control with a method for dealing with the dimensionality curse. For most frequently used models, the kernel mapping offers a unifying foundation.

Shan et al. [24] Finding diseased tissues and segmenting them from CT slices is difficult due to comparable neighboring tissues, ambiguous boundaries, and unpredictable infections. To overcome these challenges, Author presented a 2-route convolutional neural network (CNN) for identifying and categorizing COVID-19 infection on Computed tomography scans using global and local characteristics extracted from the images. Each pixel in the image is divided between normal and diseased tissues. To improve accuracy rate, utilized 2 alternative techniques to describe the input image: fuzzy -means clustering with local directional pattern, (LDN) encoding approaches. As a result, extract more complicated patterns from the image. An augmentation technique is used to address overfitting issues caused by limited samples. The findings showed that the suggested framework had an accuracy of 96%, recall of 97%, score of 97%, an average surface distance (ASD) at 2.8(+.3 or -.3) mm, and a volume overlap error (VOE) around 5.6(+1.2% or -1.2%).

Selvaraj et al. [25] presented a Deep Neural Network model for COVID-19 identification from a CT axial view image of the lung. To retrieve the specific details from the CT scans, the suggested approach was using the ZM for shape feature with GLCM for texture features, as well as specific-region for choosing the training sites. Our approach provides a reliable method for detecting COVID-19 virus in the lungs, as well as a tool for radiologists that determine the infection stage and percentage. With a restricted amount of training points, Model produced superior outcomes. While, Sensitivity-Specificity, EM, and Sm, the overall average dataset performance was 70 percent, 94 percent, 86 percent, and 78 percent, respectively. In

contrast to many other prominent DNN such as U-Net, Gated-U Net, like Dense-U Net, U-Net++ and Inf-Net, or Semi-U Net, the suggested approach improves average performance in case of Sensitivity, Specificity, Dice, and EM by 10.9 percent, 26 percent, 24.7 percent, and 16.5 percent, respectively. Furthermore, to maintain model performance, these prominent DNN need a greater number of images in the training datasets. The suggested model performed much better with a lot lower amount of training points there in training dataset.

Some of the application of image processing are illustrated in table 1.

Table 1. COVID-19 Infection Detection using Image Processing

Ref	**Year**	Method	**Description**	**Results**
[6]	2021	CT scans	Best results obtained ResNet50V2, the modified feature pyramid system network with proposed architecture.	Accuracy of 98.49%
[7]	2020	x-ray	CNN model was used	Accuracy of 83.84%
[8]	2020	x-ray	By COVID-Net upon COVIDx test dataset. expedite the development of more effective accurate but practical deep learning algorithms for COVID-19 case detection using CXR images	Accuracy of 93.3%
[9]	2021	CT scan	Highest performing model (ResNet18) was selected and used. This help in the detection of COVID-19 signatures from CT scan sections of the lungs in a quick and accurate manner.	Accuracy- 99.4%, sensitivity –100%, specificity- 98.6 %
[10]	2020	x-ray	The model can diagnose COVID-19 in a matter of seconds, . Other chest-related illnesses, such as TB and pneumonia, may also be diagnosed. Without employing a feature extraction method, the model categorized chest X-ray	98.08 % Binary, 87.02% multi-class tasks.
[12]	2021		Using the reflecting loss distance here between actual data sample space as well as the produced data, the suggested semi supervised approach achieved reliable classification.	Accuracy -94%, sensitivity-96%, specificity - 92%.
[13]	2020	X-ray	As a result, the suggested method is effective in detecting COVID19 throughout X-ray images. Mobile Net architecture with the SVM classifier using a linear kernel gives 98.5%.	Accuracy of 98.5% For Mobile Net architecture with the SVM & 95.6% for DenseNet201 with MLP.
[14]	2020	CT scan	By using CTSI of the coronal but also axial-view datasets, this study suggested	Average infection rate of 38.52% and

			preliminary research to investigate the COVID-19 infection.	39.06%, with axial-view (10 slices) and coronal-view resp.
[15]	2020	CT scan	The CT visual quantitative study has a high level of consistency and can accurately represent the COVID-19 clinical categorization	82.6% - Sensitivity and 100% - specificity
[16]	2020	x-ray	Dense Net models excellent by f1-scores of 0.89 - 0.91, InceptionV3 model poorest with f1-scores around 0.67 - 0.00 for common and COVID-19, respectively.	Accuracy of 90% -
[17]	2020	CT scan	The Inf-Net and Semi-Inf-Net segmentation models exceeds the leading segmentation models. The suggested approach can distinguish between infections as well as normal tissue by detecting items with low intensity contrast.	
[18]	2020	x-ray	The DenseNet201 deep CNN outperforms the other 3 CNN	Classification Accuracy : Normal vs. Pneumonia=98% Bacterial vs. Viral pneumonia=95% Normal vs. bacterial vs. Viral pneumonia=93.3%
[19]	2019		With retrieved ROI, characteristics contrast correlation, Mean, homogeneity, variance, standard deviation, and kurtosis are extracted, to identify lung infection.	Efficient – 94.5% Sensitive – 74.2% Specific – 77.6% Recall – 66.3%
[20]	2020	CT scan	COVID-19 can be detected and distinguished from community-acquired pneumonia and other lung illnesses using a deep learning algorithm.	Sensitivity – 90% Specificity – 96% AUC- 0.96
[21]	2021	CT scan	Visualize the diseased region and keep an eye on the disease's progression. Furthermore, given low-intensity contrast between lesions and healthy tissue, the suggested method may identify aberrant areas.	Accuracy – 98% Precision – 71% Dice – 57% Sensitivity – 73% F-Measure – 71% MCC – 71%

3. Application of Image Processing for Other Lung Infection Detection

CT image segmentation of Lung is a required first step in lung image analysis and is required for successful lung CT image analysis, including lung cancer diagnosis [26]-[28].

Hasan et al. [29] presented a combined method for automated diagnosis of pneumonia with chest X-ray images utilizing Image Processing, a version of VGG-16 and VGG-19, as well as transfer learnt InceptionResNetV2 model independently, 3 types of Deep Convolutional Neural Network CNN. To test model, utilized the Mendeley OCT with Chest X-Ray dataset, as well as a portion of the CXR-14 chest x-ray input data. Achieved 96.07 percent accuracy with the VGG-16 model, 94.88 percent with the VGG-19 model, and 96.07 percent with the transfer learned InceptionResNetV2 model, each of which beat the transfer learned InceptionV3 benchmark framework on the Mendeley OCT with Chest X-Ray dataset. The F1-scores for VGG16, VGG-19, and InceptionResNetV2 models for the slice of CXR-14 datasets are 68.84 percent, 73.66 percent, and 73.42 percent, respectively, while VGG19 and InceptionResNetV2 beat ResNet50 model, that has an F1-score of 71.8 percent.

Samuel et al. [30] described a technique for improving TB diagnostic specificity image-processing of lung captured images through normal x-ray and those obtained via sputum smear microscopy. A basic framework is created first, followed by a process to extract relevant imaging characteristics for use in reliable characterization of latent, active, drug-resistant, as well as TB-free samples. First, Effective Image Processing of Chest X-ray Images Using CAD, Secondly Analyzing Images Produced by Sputum Smear Microscopy Requires Robust Image Processing includes marking, image processing, segmentation of bacilli, bacilli classification. These characteristics of performance include: Greater than 70% sensitivity; more than 98 percent specificity; Simplicity, which may be readily given by a technician with little or no experience; Required equipment and reagents; stability with a two-year shelf life; and cost no more than the present test.

Norval et al. [31] used Convolutional Neural Networks to test the accuracy of two techniques for detecting pulmonary tuberculosis based on patient chest X-ray images (CNN). A hybrid technique was also explored, combining the original statistical computer-aided detection approach of Neural Networks. A total of 406 normal and 394 aberrant images were used in the simulations. Based on the simulations, a clipped area of interest combined with contrast enhancement produces good results. Even greater results are obtained when the images are further enhanced using the hybrid technique. The ROI is taken from the preprocessed image collection after it has been subjected to even further processing. For some more consistent overall accuracy, a fixed random generator is used again here. The technique is a hybrid of computer-aided detection (CAD) with DCNN stages. The lung (ROI) is extracted and supplied as a datasets into the DCNN. The findings indicate that image preprocessing improves accuracy when compared to no preprocessing. The primary benefit of the hybrid approach is substantially higher accuracy by minimizing over-fitting. Extracting just the ROI from these images gives even better results, with a great accuracy of 92.54 percent.

Ayan et al. [32] evaluated the performance of 2 CNN networks in diagnosing pneumonia illness. Utilized transfer learning with finetuning when training model. Compared 2 network tests outcomes after the training stage. The Vgg16 network outperformed the Xception network in terms of accuracy 0.87 percent, specificity 0.91 percent, pneumonia precision 0.91 percent, as well as pneumonia f1 score 0.90 percent, according to the test findings. While the Xception network beats the Vgg16 network by 0.85 percent in

sensitivity, 0.86 percent in normal precision, but also 0.94 percent in pneumonia recall. Each network does have its unique detection capacity on the datasets. The Xception network outperforms the Vgg16 network in identifying pneumonia patients. Simultaneously, the Vgg16 network is better at identifying normal instances.

Bharati et al. [33] used Marker-Controlled Watershed with Region Growing, then Marker-Controlled Watershed covering to develop and evaluate 3 image segmentation methods for investigating lung cancer. The results show that the Marker-Controlled Watershed with Covering offers the best enactment in terms of separation result and organization time. As a result, during the image segmentation phase, we used it. Furthermore, we use a color feature for the investigation of lung cancer through binarization mostly in extraction of such feature together in stage. Finally, the binarization method was successful in resolving the lung's condition (cancer/normal) out from CT scan image. Using the test as well as train LIDC data sets, this study developed Random Forest Ensemble with RUS Boost. Lobulation. According to RUS Boost, Spiculation and Texture offer the best accuracy when testing datasets. For the training dataset, however, Texture has the greatest accuracy while Spiculation has the second highest accuracy.

Perumal et al. [34] used image processing to identify lung cancer on CT scan images, which enhances the quality of the processed lung images and allows for early disease diagnosis. Utilizing Gabor filter image processing, the raw input image, which is often noisy, is greatly improved. The area of interest is recovered from lung cancer images using Otsu's threshold segmentation technique and the 5-level HAAR wavelet transform method, which are both fast and accurate. The suggested Enhanced Artificial Bee Colony Optimization (EABC) is used to identify cancer suspicious areas in CT scan images. The suggested EABC implementation component makes use of CT (Computer Tomography) scanned lung images in conjunction with the MATLAB software framework. The total time spent on the procedure is significantly reduced. This technique may help radiologists and medical professionals identify syndromes in their early stages and avoid the more severe phases of malignancy. Using CT scan images of the lungs with a high degree of sensitivity and a reasonable number of false positives per image (92 percent sensitivity and 0.04 false positives every image).

Garstka & Strzelecki [35] presented a self-constructed CNN developed on a very modest dataset for lung X-Ray image categorization. This article proved that conventional CNN is capable of providing very good classification (85 percent) of X-ray pneumonia images when faced with a real three-class issue (differentiating among viral, bacterial & control cases). In addition, among other methods, the maximum responsiveness was found (0.95). It is critical in screening testing, when detecting the greatest number of positive cases is critical. The observed findings are encouraging and indicate the efficacy of the suggested approach of input data augmentation relies on geometric image modifications. Following further refinement, the approach provided in this paper might be used to augment the interpretation of X-ray pneumonia images in paediatric patients in the future.

Sharma et al. [36] described an unique method for identifying the existence of pneumonia clouds within chest X-rays (CXR) that relies only on computer vision techniques. Researchers worked on 40 analogue chest CXRs from normal and Pneumonia-infected individuals for this. For trimming and extracting the lung area from images, unique algorithms were created. To recognize pneumonia clouds, we utilized Otsu thresholding, which separates the healthy section of the lung out from cloudy parts afflicted with pneumonia. Researchers had recognized the lung region using rib cage border identification and

computed its area. Inside the lung region, they also utilized Otsu thresholding to separate the pneumonia cloud out from healthy lung.

Varshni et al. [37] presented a study to increase medical proficiency in places where radiotherapists are still few. In such distant regions, this research can help with the early detection of Pneumonia and therefore avoid negative effects (including mortality). So far, little effort has been done particularly to detect Pneumonia using the aforementioned dataset. Researchers evaluated the effectiveness of several pre - trained models Convolutional networks alongside distinct classifiers, and eventually chose DenseNet-169 for the feature extraction phase and SVM for the segmentation process based on statistical data.

Tilve et al. [38] focused on assessing and analyzing the identification of lung illness using various computer-aided approaches, and it proposed a new model for identifying pneumonia, which would be utilised in future research. In this survey, researchers attempted to become acquainted with the various image pre-processing methods being used transform raw X-ray image data into standard formats for identification and processing, as well as machine learning based methods such as Convolutional Networks, RESNET, CheXNet, DENSENET, Artificial Neural Networks, and KNN, which is an essential step in accurately detecting pneumonia.

Ayan & Ünver [39] examined the performance of two Convolutional Neural Networks in diagnosing pneumonia illness. They employed transfer learning and refining when training the model. Following the training stage, they compared the outcomes of two network tests. According to the test findings, the Vgg16 network beats the Xception system in terms of accuracy 0.87 percent, specificity 0.91 percent, pneumonia precision 0.91 percent, and pneumonia f1 score 0.90 percent. While the Xception network surpasses the VGG16 network in terms of sensitivity (0.85%) ordinary precision (0.86%), and pneumonia retention (0.94%). The Xception network outperforms the VGG16 network in identifying pneumonia patients. Simultaneously, the VGG16 network is better at identifying ordinary instances.

Li et al. [40] compared radiologists' capability to detect focal pneumonia using conventional chest radiographs alone vs standard + bone-suppressed chest radiographs. An investigator research comprised 36 patients with 46 focal airspace opacities owing to pneumonia (10 sufferers had bilaterally opacities) and 20 patients lacking focal opacities. The bone suppression image analysis technology was used to produce matching bone suppression images from the 56 radiographs. Depending on 46 positive lungs as well as 66 negative lungs, the average value of the region under the ROC curve (AUC) for eight spectators increased considerably from 0.844 with conventional images alone to 0.880 with standard + bone suppression images ($P < 0.001$).

Poornimadevi & Helen Sulochana [41]described an automated identification of TB in lung images. The position of TB in the lung varies based on the stage of infections and the patient's age. Because the X-ray images show varying lung geometries, a static model is insufficient to explain the lung areas. Using stiff registrations, researchers linearly align entire training masks to a set of input CXRs. For the input CXR, the mean mask calculated on a subset of all the most comparable training masks is employed as an approximation lung model. The watershed categorization is used to classify an approximation model. Furthermore, the wiener filter and histogram equalization are used to increase the accuracy of the categorization findings. The suggested technique is tested using the JSRT and MC datasets.

Panicker et al. [42] reviewed several image processing algorithms used to detect M. tuberculosis through microscopic sputum images. For such investigation, the approaches developed for both traditional and fluorescent microscopes in the previous two decades were taken into account. Researchers present a survey of automated approaches based on image processing techniques that were disclosed between 1998 and 2014. The review demonstrates that the precision of algorithms for the automated diagnosis of tuberculosis has grown tremendously over the years, and it joyfully notes that commercial products rely on published studies have also begun to come on the market. This review may be beneficial to scholars and practitioners engaging in the topic of TB automation, since it provides a thorough and approachable perspective of methodologies used in this field of study.

Liu & Alcantara [43] proposed a unique technique for using CNN models to identify and categorise tuberculosis symptoms in X-ray images. The study described here is the first to use CNN for TB identification in a large TB dataset. They apply a series of optimization techniques to further increase the precision based on the study results and the unique technological challenges in this big imbalanced, less-category dataset. This technique demonstrates the stability and universality of CNN models.

Hooda et al. [44] suggested a TB detection technique based on deep CNN employing CXRs. Because CNN identifies the most discriminative information autonomously based on the desired objective, the use of manually generated features has decreased. Researchers presented a CNN network that accurately classifies CXR images into TB positive and negative groups. They also examined the effectiveness of 3 distinct optimizers.

Saravanan et al. [45] determined the efficiency of TB detection employing image classification approaches. Numerous techniques are used in image segmentation, such as adaptive colour thresholding classification, clustering, adaptive filtering, ANN, graph cut segmentation, genetic algorithms, SVM, random forest learning, seeded region growing methodology, image enhancement, and so on. The neural Networks approach gives the greatest outcomes of any technology used to detect tuberculosis. This study presents a literature review on the detection of tuberculosis (TB) using image processing method.

Shabut et al. [46] described a smart phone-based mobile enabled plasmonic relies on ELISA TB antigen-specific antibody detection method that used machine learning approaches. The system can identify samples (wells) without the use of a guideline or virtual plate by employing a strong image processing approach composed of clustering and objects identification. The decisions elements aided in the selection of the correct cluster from a large number of clusters, the identification of wells, and the separation of data from noise. As a result, unlike the stated articles, the method does not necessitate the user providing seed points or cropping. Furthermore, the system can read numerous samples and identify them as negatively or positively in real time. Positive and negative samples are coloured using the plasmonic ELISA method. Therefore, making a final selection solely on colour look is not always accurate. As a result, researchers showed a smartphone-based POC platform that makes the ultimate choice depending on colour analysis in this study. This study used supervised machine learning to remove the TB test results from individual colour vision and explanation subjectivity. Using the Random Forest classifier plus 18 histogram characteristics, they achieved 98.9 percent accuracy.

Some of the application of image processing on other lung infections are illustrated in table 2.

Table 2. Lung Infection Detection using Image Processing

Ref	Year	Infection Type	Method	Description	Result
[26]	2018	Lung and thorax	X-ray, CT scans, MRI, PET	The lung disease stage may be determined accurately by calculating the tumor's measures, d to discover the irregularity issues in target images	Accuracy of 90%. While there are just 0.05 false positives per image.
[29]	2019	X-ray	Pneumonia	VGG-16, VGG-19 and InceptionResNetV2 to identify pneumonia that outperformed InceptionV3 by 3.3 percent.	VGG-16 - 96.07% VGG-19 - 94.88% InceptionResNetV2 – 96.07%
[30]	2018	x-ray	Tuberculosis	Sputum - Simple; easy to interpret; less expensive; good specificity. Chest x ray- Quick; no need of specimen.	Sputum Smear Microscopy: Sensitivity =+70% Specificity =+98%
[31]	2019	x-ray	Tuberculosis	Hybrid approach gives higher accuracy by minimizing over-fitting, image preprocessing improves accuracy compared to no preprocessing	92.54% Accuracy
[32]	2019	x-ray	pneumonia	Detecting pneumonia patients, the Xception network beats the Vgg16 network. The Vgg16 network is good at identifying normal occurrences.	Vgg16 > Xception Accuracy(.87%) Specificity (.91%) F1 score (.90%) Xception > Vgg16 Sensitivity (.85%) Precision (.86%) Recall (.94%)
[34]	2018	CT scan	Lung cancer	EABC using pixel percentage identify lung cancer nodules. When compared to other current methods, the suggested methodology	92% - Sensitivity (0.04 false positives per image)

				yields more promising results.	
[35]	2020	x-ray	pneumonia	Used CNN based model to diagnose among bacterial, viral and healthy subjects.	Accuracy of 85% and sensitivity of 95%
[37]	2019	X-Ray	pneumonia	The functionality of pre-trained CNN models utilized as feature-extractors followed by different classifiers for the classification of abnormal and normal.	ResNet-50 achieved accuracy of 77%.
[39]	2020	X-ray	pneumonia	Content-based image retrieval technique was used to annotate the image using CNN.	Achieved 99% of accuracy and 98% of recall.
[46]	2018		tuberculosis	Real-time detection	Achieved 98% of accuracy

4. FDG in Inflammatory and Infectious Diseases

Acute lower respiratory tract illnesses have been among the top three leading reasons of death in both people of all ages for generations, putting a significant strain on the healthcare system. Although traditional radiography imaging methods, such as chests X-ray (CXR) and computed tomography (CT), are indeed the predominant imaging modalities for diagnosing respiratory infection, FDG-PET/CT has demonstrated to be helpful in circumstances when traditional imagery fails. Metabolic imaging could not only detect and monitor contamination sooner than that of other methods, but might also offer crucial structural information.

This modality's great sensitivities, along with its larger anatomical covering, results in a much more thorough and full evaluation of the person's major disease load, enabling for yet more personalized care strategies.

Although FDG-PET/CT imaging was already largely used to image malignancy, numerous writers had acknowledged its use in non-neoplastic diseases including lung infections. It’s because FDG works as a glucose analog and is consequently taken up by the body via glucose transporter 1. (GLUT-1). FDG is phosphorylation either by rate-limiting enzymes hexokinase after intracellular absorption, locking FDG-6-phosphate with in cells. FDG-PET/CT may detect areas with elevated glucose usage and metabolic, that are non-specific but frequent indicators of infections, inflammatory, and malignancy.

Finally, integrating the functionalities of FDG-PET/CT also with structural/anatomic components of Tomography does have the power to transform lung infection detection and therapy. FDG PET/CT imaging has huge advantages if apply in conjunction with the other imaging technologies in respiratory infections procedures, because it offers specific data on the cellular scale and can precisely evaluate disease. Though it is not ordinarily seen as a stand-alone research method in respiratory infections procedures, it has high relevance if used in conjunction with the other imaging technology.

Approximately 170 million individuals have been impacted by the worldwide COVID-19 catastrophe, which was triggered by the acute respiratory distress sickness coronavirus-2 (SARS-CoV-2). Thousands of patients have had lung signs acute enough just to necessitate hospitalizations and sequential radiography. Whereas the principal diagnostic methods were reversed transcription-polymerase chain reaction (RT-PCR) Computed tomography and, less usually, chest CT, FDG-PET/CT may accidentally uncover undetected instances of COVID-19 in the initial phase of the illness, while signs are vague. In asymptomatic patients, incidental FDG-PET/CT findings have been published in recent research, validating COVID-19.

Bai Y et al. [47] evaluated metabolism rate in affected sections of people hospitalized from acute COVID-19 virus using [18F] fluorodeoxyglucose positron emissions tomography/computed tomography (PET/CT). Seven recovering in hospital individuals diagnosed with severe COVID-19 virus in an investigation was aimed. These individuals had received 2 sequential negative reverse transcriptase polymerase chain reaction (RT-PCR) findings for SARS-CoV-2 nucleic acid prior to FDG PET/CT. Medical intake was completed, which included signs, therapy, test findings, and follow-up. COVID19 patients' PET/CT images were incorporated in the study of patient populations who were of same gender and age. Following two subsequent false RT-PCR examinations in people hospitalized from acute COVID-19 virus, FDG PET/CT quantitatively findings show that considerable inflammatory area persisted in the bronchi lungs, mediastinal lymphoid tissue, spleen, and liver. Average CT intensity, Standard uptake value and maximum CT intensity and Standard uptake value is evaluated and it was found that among all spleen has maximum value of maximum standard uptake value and liver and lymph node has highest values for SUV average. For spleen maximum standard uptake value is 0.863 for p=0.0030 and SUV average for liver is 0.7970 with p=0.0070.

Martinez RB et al. [48] detected Covid-19 infections that are clinically undetected in order to prevent community transmission. 492 18-FDG-PET/CT Anomalies in the lungs and throughout the body were examined using PET/CT imaging. Covid-19 virus was verified in 13/29 individuals by a nasopharyngeal nucleic acid PCR tePure ground-glass opacity (GGO) was the most prevalent lung abnormality (90%) in periphery dispersion (100%), affecting one lobe in cases (30.8%), two–three lobe in cases, and 4-5 lobule in cases (38.4 percent). SUV_{max} was 4.7 on average (range 1.3–13.1). Within 6.4–7.8 days (range 1–24), ten patients experienced symptoms, primarily fever, tiredness, and a dry cough. 8 of the 12 cases with accessible lab results had lymphopenia, while 5 acquired neutrophilia. 5 of the patients needed to be hospitalized, and 2 of them passed away of the symptoms. Unexpected anomalies on nonurgent radiography therapy that are symptomatic of Covid-19 pneumonia are evaluated in cases, along with diagnosis, laboratory, and epidemiological studies, to ensure proper diagnosis and prophylactic measures. Measures for giving therapy and reducing the danger of infection are crucial for protecting vulnerable individuals and hospital staff from Covid-19 illness. As a result, it's not shocking to discover it in asymptomatic people who are being examined for other reasons. More to minimize SARS-CoV-2 transmission, it is critical to recognize its symptoms and implement efficient mitigation strategies, particularly among vulnerable groups, such as the elderly and those with comorbidities.

Jacobi A et al. [49] presented the most obvious symptoms and forms of pulmonary abnormalities on Chest radiograph in COVID -19 so that health doctors can better tackle the epidemic. On traditional chest radiographs and also chest CT, signs of COVID -19 respiratory illness can be observed. In describing cases with or accused of having COVID -19 on CXR, phrases like irregular, patchy, hazy, reticular, and extensive ground glass opacities are common. It is indeed crucial to inform clinicians about the severity of the disease based on total lung involvement. Because of its ubiquitous availability and decreased infection prevention and control difficulties that presently limit CT use, the medical profession will increasingly rely on portable CXR as the pandemic unfolds. When compared to CT, CXR is less sensitive in detecting COVID -19 lung disease, with an estimated baseline sensitivity of 69 percent.

Kim et al. [50] compared the operational metabolic imaging results of 18F-fluoro-2-deoxy-D-glucose (FDG) positron emission tomography (PET)/computed tomography (CT) in patients with early stage and non-invasive lung aspergillosis (IPA and NIPA, respectively). Researchers looked at 24 cases who had lung aspergillosis and had an 18F-FDG PET/ CT scan to assess a lung mass or a fever of unclear cause. Eight of the 24 individuals were diagnosed with IPA, while the other 16 were identified with NIPA. Cases was of younger (48 years vs. 62 years), and immunocompromised circumstances were much more common in these cases (88 percent vs 6 percent). Numerous lesions have been found in 50% (4 of 8) and 19% (3 of 16) of IPA and NIPA patients, including both, and the excitable metabolic nodule pattern (6 of 8 patients, 75%) and the isometabolic halo pattern (8 of 16 patients, 50%) were the most common patterns on 18F-FDG PET/CT in IPA and NIPA patients, respectively. In IPA patients, the isometabolic halo pattern was not seen. In IPA and NIPA, the median SUVpeak was 4.5 (range, 1.3Y8.9) and 1.6 (range, 0.5Y3.1), respectively.

Qin et al. [51] explained the 18F-FDG PET/CT findings of 4 cases hospitalized with breathlessness as well as fever when the COVID-19 epidemic was still unidentified and the bacteria's pathogenicity was unclear. The goal of this case reports is to show the 18F-FDG PET/CT outcomes in patients with COVID-19-induced severe respiratory illness in Wuhan, Hubei Province, China. A study of the sufferers' health records, clinical and biochemical data, and imaging findings clearly showed that COVID-19 was the diagnostic. In much more than two lung chambers, all of the case developed periphery ground-glass opacities and/or lung restructurings. There were indications of lymph node dissection and a significant 18F-FDG uptake in the lung lesions. Disseminated illness, on the other hand, was not present, indicating that COVID-19 has pulmonary tropism. Although 18F-FDG PET/CT cannot be utilized in an emergency situation and is not indicated for infectious disorders, our preliminary findings suggest that this imaging technology could be useful in the differential diagnosis of difficult situations. The SUV_{max} ranges from 4.6-9.3 in the four cases.

Zou S et al. [52] examined for 5 days, a 55-year-old male smoker in Wuhan, China, suffered with sporadic fever, weariness, and a chronic cough. An outside institution's preliminary chest CT results revealed lung cancer. Further examination was done using fluorine 18 fluorodeoxyglucose (FDG) PET/CT. In the right lung, the PET maximum peak projected image revealed an FDG-avid bulk with a maximal standardized uptake value of 4.9. FDG levels were found to be higher in the right paratracheal and right hilar lymph nodes, and also in the bone marrow. Ground-glass opacities with focal consolidation predominantly in the right upper lobe and a focal opacity in the left upper and right middle lobes were seen on axial imaging. Nasopharyngeal swab tests were used to rule out influenza, respiratory syncytial virus, and other common respiratory viral infections. Four days later, a follow-up CT indicated development of lesions in the bilateral upper and middle lobes, as well as new focal opacities in the left upper and lower lobes. SARS coronavirus

2 infection was confirmed by real-time fluorescence polymerase chain reaction a week later, confirming coronavirus illness 2019. (COVID-19). The patient was discharged after 10 days of treatment since he had healed from COVID-19.

Cristina et al. [53] explored the association between metabolic and structural changes of lung parenchyma in asymptomatic cancer patients with suspected COVID-19 pneumonia, as a potential added diagnostic value of fluorine-18 fluorodeoxyglucose (18F-FDG) positron emission tomography-computed tomography (PET/CT) scans in this subpopulation. CT signs classified as CO-RADS category 5 or 6 were found in 16/41 (39%) oncological patients derived to multimodal PET/CT imaging. SUV max was higher in patients with CO-RADS 5 and 6 vs. 4 (6.17±0.82 vs. 3.78±0.50, p=0.04) and vs. 2 and 3 categories (3.59±0.41, p=0.01). A specificity of 93.8% (IC 95%: 71.7-99.7%) and an accuracy of 92.9% were obtained when combining a CO-RADS score 5-6 with a SUV max of 2.45 in pulmonary infiltrates. In asymptomatic cancer patients, the metabolic activity in lung infiltrates is closely associated with several combined tomographic changes characteristic of COVID-19 pneumonia. Multimodal 18F-FDG PET/CT imaging could provide additional information during early diagnosis in selected predisposed patients during pandemic. The prognostic implications of simultaneous radiological and molecular findings in cancer and other high-risk subpopulations for COVID-19 pneumonia deserve further evaluation in prospective researches. 18F-FDG PET/CT studies is closely associated with several tomographic changes characteristic of COVID-19 pneumonia. Multimodal 18F-FDG PET/CT imaging could provide additional information during the diagnosis of COVID-19 in selected patients, even in early stages of the disease.

Randy Yeh et al. [54] performed a single institution retrospective review of patients diagnosed with COVID-19 using real time reverse transcription–polymerase chain reaction (RT-PCR) who underwent FDG PET/CT for routine cancer care between March 1, 2020 to April 30, 2020, during the height of the pandemic in New York City, Patients with positive FDG PET/CT scans were more likely to be symptomatic and require hospitalization. The incidental detection rate of COVID-19 on FDG PET/CT is relatively low (41.9%) in patients with laboratory-confirmed infection. For positive scans, PET and CT findings were recorded, including location, FDG avidity (SUV max) and CT morphology. Patient demographics and COVID-19 specific clinical data were collected and analyzed with respect to PET/CT scan positivity, lung SUVmax, and time interval between PET/CT and RT-PCR.

Extra: Patients with positive scans had significantly higher rates of symptomatic COVID-19 infection (77% vs 28%, p = 0.01) and hospitalizations (46% vs. 0%, p = 0.002) compared to patients with negative scans. Eleven of 13 patients (84.6%) with positive scans had FDG-avid lung findings, with mean lung SUV max of 5.36. Six of 13 patients (46.2%) had extrapulmonary findings of FDG-avid thoracic lymph nodes. The detection rate was significantly lower when the scan was performed before RT-PCR versus after RT-PCR (18.8% (n = 3/16) vs. 66.7% (n = 10/15), p = 0.009). Lung SUV max was not associated with COVID-19 symptoms, severity, or disease course. FDG PET/CT has limited sensitivity for detecting COVID-19 infection. However, a positive PET scan is associated with higher risk of symptomatic infection and hospitalizations, which may be helpful in predicting disease severity.

Setti et al. [55] proposed The study aimed to compare the incidence of interstitial pneumonia on [18F]-FDG PET/CT scans between two 6-month periods: (a) the COVID-19 pandemic peak and (b) control period. Secondly, we compared the incidence of interstitial pneumonia on [18F]-FDG PET/CT and epidemiological data from the regional registry of COVID-19 cases. Additionally, imaging findings and the intensity of

[18F]-FDG PET/CT uptake in terms of maximum standardized uptake value (SUV max) were compared. To evaluate the differences between the two symmetric groups (period of COVID-19 pandemic and control), the stratified Cochran–Mantel–Haenszel test was used. Chi-square test or Fisher's exact test and t test or Wilcoxon test were performed to compare the distributions of categorical and continuous variables, respectively. Significant increase of interstitial lung alterations at [18F]-FDG PET/CT has been demonstrated during the COVID-19 pandemic. Overall, 1298 patients were included in the study. Signs of interstitial pneumonia were observed in 24 (4.2%) and 14 patients (1.9%) in the COVID-19 period and the control period, respectively, with a statistically significant difference ($p = 0.013$). The level of statistical significance improved further when the period from January to May was considered, with a peak in March (7/83 patients, 8.4% vs 3/134 patients, 2.2%, $p = 0.001$).

Fu et al. [56] A 48-year-old woman presented with 10-day history of cough and fever (up to 39.1 °C). Nasopharyngeal swab specimen was positive for COVID-19 nucleic acid test (RT-PCR). The patient was effectively relieved from clinical symptoms and was negative in two subsequent RT-PCR tests (day 13, day 14). [18F] FDG PET/CT scan (day 16) was performed to evaluate any other active disease process. It showed multiple FDG-positive consolidative opacities in both lungs (PET, fusion; SUV max ranged 2.7–5.9) and multiple FDG-avid lymph nodes in the left subclavian, mediastinum, and hilum regions (arrows, fusion; SUV max ranged 2.9–6.5). FDG uptake may vary with different stages of virus and disease . FDG PET/CT with its capability of directly mapping the location and activity of inflammation during virus exposure may have a role to play when there is uncertainty of diagnosis, for clinical management and for monitoring the effect of treatment.

Bahloul et al. [57] study aimed to identify specific COVID-19 18F-FDG-PET signs in patients that were (i) suspected to have a lung infection based on 18F-FDG-PET/CT recorded during the COVID-19 outbreak and (ii) whose COVID-19 diagnosis was definitely established or excluded by appropriate viral testing. Twenty-two consecutive patients referred for routine 18F-FDG-PET/CT examinations during the COVID-19 outbreak (March 25th to May 15th 2020) and for whom CT slices were evocative of a lung infection were included in the study. Eleven patients were confirmed to be affected by COVID-19 (COVID+), whereas the other eleven patients were not (COVID−) and were predominantly suspected of having bacterial pneumonia. CT abnormalities were not significantly different between COVID+ and COVID− groups, although trends toward larger CT abnormalities ($p = 0.16$) and lower rates of consolidation patterns (0.09) were observed in the COVID+ group. The maximal standardized uptake values (SUV max) of lung areas with CT abnormalities were however significantly lower in the COVID+ than the COVID− group (3.7 ± 1.9 vs. 6.9 ± 4.1, $p = 0.03$), with the highest SUVmax consistently not associated with COVID-19. Among CT abnormalities evocative of lung infection, those related to COVID-19 are associated with a more limited 18F-FDG uptake. This observation may help improve our ability to detect COVID-19 patients.

Some of contribution of researchers in FDG-PET/CT images analysis-based lung infection detection are presented in below table 3.

Table 3. Research Contributions in FDG-PET/CT Images based Lung Infection Detection

Ref	Year	Method	Results

[47]	2021	18-FDG-PET/CT	Spleen standard uptake value (SUV_{max})= is 0.863 for p=0.0030 and $SUV_{average}$ =0.7970 for liver is with p=0.0070.
[48]	2021	18-FDG-PET/CT	SUV_{max} = 4.7 range from 1.3–13.1
[49]	2020	CXR- Chest radiograph	When compared to CT, CXR is less sensitive in detecting COVID -19 lung disease, with an estimated baseline sensitivity of 69 percent.
[51]	2020	18F-FDG PET/CT	SUV_{max}=4.6-9.3 in the four cases
[52]	2021	fluorine 18 fluorodeoxyglucose (FDG) PET/CT	SUV_{max}=4.9
[53]	2021	18F-FDG PET/CT	SUV_{max} = 2.45
[54]	2021	18F-FDG PET/CT	SUV max of 5.36
[56]	2020	18F-FDG PET/CT	2.7–5.9
[57]	2021	18F-FDG PET/CT	3.7 ± 1.9 vs. 6.9 ± 4.1

5. Limitations and Future Research Directions

- There are unlimited opportunities for the improvement of the Lung Infection detection through the use of deep learning-based systems.
- AI and ML have the potential to transform the way Medical Imaging is advancing, with AI and ML solutions complementing the work of physicians to enable the development of new treatment paradigms.
- Blockchain is the area with the fastest growth and is worth watching because the secure distributed storage of medical data outside medical institutions is a precondition for enabling patients to have access to and control of their data.
- 3-D visualization technologies allow physicians to "see" the patient in new ways, with greater precision that supports more effective treatments and better clinical outcomes.

6. Conclusion

This paper provides an overview of the integration of Deep Learning with Medical Imaging (CT scan/MRI/ FDG-PET/CT) in various infectious and inflammatory diseases, not only in the setting of diagnosis but also in the evaluation of treatment efficacy as learning has gained a central position with regard to the automation of our daily life and has delivered considerable improvements in comparison with traditional machine learning algorithms. Based on their tremendous performance, most researchers believe that, within next 15 years, deep learning-based applications will take over from humans in certain roles and that most daily activities will be performed by autonomous machines. Many big research organizations are working on deep learning-based solutions that encourage the application of deep learning on medical images. Looking to the brighter side of machine learning, we are hoping that humans will soon be replaced in most medical applications, especially diagnosis. However, we should not consider it as the only solution; there are several challenges reducing the expansion of deep learning. One of the major barriers is the unavailability of

annotated datasets. Thus, it remains to be seen whether we will be able to obtain enough training data, without which the performance of deep learning algorithms will be affected. Recent developments on other applications have shown that the bigger the data, the better the result; however, how much big data could be used in health care. So far, deep learning-based applications have provided positive feedback. However, due to the sensitivity of health care data and a variety of challenges, we should look at more sophisticated deep learning methods that can deal with complex health care data efficiently. We conclude that using deep learning-based algorithms to enhance Lung Infection diagnosis opens up an infinite number of possibilities.

References

[1] C. F. J. Kuo et al., "Automatic lung nodule detection system using image processing techniques in computed tomography," Biomed. Signal Process. Control, vol. 56, p. 101659, Feb. 2020, doi: 10.1016/J.BSPC.2019.101659.

[2] A. A. Abdulmunem, Z. A. Abutiheen, and H. J. Aleqabie, "Recognition of corona virus disease (COVID-19) using deep learning network," Int. J. Electr. Comput. Eng., vol. 11, no. 1, pp. 365–374, Feb. 2021, doi: 10.11591/IJECE.V11I1.PP365-374.

[3] S. Akram, M. Y. Javed, U. Qamar, A. Khanum, and A. Hassan, "Artificial Neural Network based Classification of Lungs Nodule using Hybrid Features from Computerized Tomographic Images," Appl. Math. Inf. Sci, vol. 9, no. 1, p. 183, 2015, doi: 10.12785/amis/090124.

[4] D. Shen, G. Wu, and H.-I. Suk, "Deep Learning in Medical Image Analysis," Annu. Rev. Biomed. Eng., vol. 19, p. 221, Jun. 2017, doi: 10.1146/ANNUREV-BIOENG-071516-044442.

[5] O. Furat et al., "Machine Learning Techniques for the Segmentation of Tomographic Image Data of Functional Materials," Front. Mater., vol. 0, p. 145, Jul. 2019, doi: 10.3389/FMATS.2019.00145.

[6] M. Rahimzadeh, A. Attar, and S. M. Sakhaei, "A fully automated deep learning-based network for detecting COVID-19 from a new and large lung CT scan dataset," Biomed. Signal Process. Control, vol. 68, p. 102588, Jul. 2021, doi: 10.1016/J.BSPC.2021.102588.

[7] S. Hassantabar, M. Ahmadi, and A. Sharifi, "Diagnosis and detection of infected tissue of COVID-19 patients based on lung x-ray image using convolutional neural network approaches," Chaos, Solitons & Fractals, vol. 140, p. 110170, Nov. 2020, doi: 10.1016/J.CHAOS.2020.110170.

[8] FA: Hersh F. Mahmood, Hooshang Dabbagh, Azad A. Mohammed, Comparative study on using chemical and natural admixtures (grape and mulberry extracts) for concrete, Case Studies in Construction Materials, Volume 15, 2021,

[9] Kumar, S. (2022). A quest for sustainium (sustainability Premium): review of sustainable bonds. Academy of Accounting and Financial Studies Journal, Vol. 26, no.2, pp. 1-18

[10] Allugunti, V.R. (2019). Diabetes Kaggle Dataset Adequacy Scrutiny using Factor Exploration and Correlation. International Journal of Recent Technology and Engineering, Volume-8, Issue-1S4, pp 1105-1110.

[11] L. Wang, Z. Q. Lin, and A. Wong, "COVID-Net: a tailored deep convolutional neural network design for detection of COVID-19 cases from chest X-ray images," Sci. Reports 2020 101, vol. 10, no. 1, pp. 1–12, Nov. 2020, doi: 10.1038/s41598-020-76550-z.

[12] S. Ahuja, B. K. Panigrahi, N. Dey, V. Rajinikanth, and T. K. Gandhi, "Deep transfer learning-based automated detection of COVID-19 from lung CT scan slices," Appl. Intell., vol. 51, no. 1, p. 1, Jan. 2021, doi: 10.1007/S10489-020-01826-W.

[13] T. Ozturk, M. Talo, E. A. Yildirim, U. B. Baloglu, O. Yildirim, and U. Rajendra Acharya, "Automated detection of COVID-19 cases using deep neural networks with X-ray images," Comput. Biol. Med., vol. 121, p. 103792, Jun. 2020, doi: 10.1016/J.COMPBIOMED.2020.103792.

[14] Z. C et al., "Lung segmentation and automatic detection of COVID-19 using radiomic features from chest CT images," Pattern Recognit., vol. 119, Nov. 2021, doi: 10.1016/J.PATCOG.2021.108071.

[15] A. Oluwasanmi et al., "Transfer Learning and Semisupervised Adversarial Detection and Classification of COVID-19 in CT Images," Complexity, vol. 2021, 2021, doi: 10.1155/2021/6680455.

[16] E. F. Ohata et al., "Automatic detection of COVID-19 infection using chest X-ray images through transfer learning," IEEE/CAA J. Autom. Sin., vol. 8, no. 1, pp. 239–248, Jan. 2021, doi: 10.1109/JAS.2020.1003393.

[17] V. Rajinikanth et al., "Harmony-Search and Otsu based System for Coronavirus Disease (COVID-19) Detection using Lung CT Scan Images."

[18] K. Li et al., "CT image visual quantitative evaluation and clinical classification of coronavirus disease (COVID-19)," Eur. Radiol. 2020 308, vol. 30, no. 8, pp. 4407–4416, Mar. 2020, doi: 10.1007/S00330-020-06817-6.

[19] E. E.-D. Hemdan, M. A. Shouman, and M. E. Karar, "COVIDX-Net: A Framework of Deep Learning Classifiers to Diagnose COVID-19 in X-Ray Images," Mar. 2020, Accessed: Oct. 30, 2021. [Online]. Available: https://arxiv.org/abs/2003.11055v1.

[20] D. P. Fan et al., "Inf-Net: Automatic COVID-19 Lung Infection Segmentation from CT Images," IEEE Trans. Med. Imaging, vol. 39, no. 8, pp. 2626–2637, Aug. 2020, doi: 10.1109/TMI.2020.2996645.

[21] T. Rahman et al., "Transfer Learning with Deep Convolutional Neural Network (CNN) for Pneumonia Detection using Chest X-ray," Appl. Sci., vol. 10, no. 9, Apr. 2020, doi: 10.3390/app10093233.

[22] K. Roy et al., "A comparative study of lung cancer detection using supervised neural network," 2019 Int. Conf. Opto-Electronics Appl. Opt. Optronix 2019, Mar. 2019, doi: 10.1109/OPTRONIX.2019.8862326.

[23] L. Li et al., "Artificial Intelligence Distinguishes COVID-19 from Community Acquired Pneumonia on Chest CT," Radiology, vol. 296, no. 2, pp. E65–E71, Aug. 2020, doi: 10.1148/RADIOL.2020200905.

[24] A. Oulefki, S. Agaian, T. Trongtirakul, and A. K. Laouar, "Automatic COVID-19 lung infected region segmentation and measurement using CT-scans images," Pattern Recognit., vol. 114, p. 107747, Jun. 2021, doi: 10.1016/J.PATCOG.2020.107747.

[25] M. I. Elbakary and K. Iftekharuddin, "COVID-19 detection using image analysis methods on CT images," https://doi.org/10.1117/12.2581667, vol. 11596, pp. 937–943, Feb. 2021, doi: 10.1117/12.2581667.

[26] S. Kalaivani, P. Chatterjee, S. Juyal, and R. Gupta, "Lung cancer detection using digital image processing and artificial neural networks," Proc. Int. Conf. Electron. Commun. Aerosp. Technol. ICECA 2017, vol. 2017-January, pp. 100–103, 2017, doi: 10.1109/ICECA.2017.8212773.

[27] F. Shan et al., "Lung Infection Quantification of COVID-19 in CT Images with Deep Learning," Mar. 2020, Accessed: Oct. 30, 2021. [Online]. Available: http://arxiv.org/abs/2003.04655.

[28] Selvaraj, Deepika, Arunachalam Venkatesan, Vijayalakshmi GV Mahesh, and Alex Noel Joseph Raj, "An integrated feature frame work for automated segmentation of COVID-19 infection from lung CT images", International Journal of Imaging Systems and Technology 31, no. 1 (2021): 28-46. https://dx.doi.org/10.1002%2Fima.22525

[29] S. Balakrishnan, J. Janet, and K. S. and S. S. Rani, "An Efficient and Complete Automatic System for Detecting Lung Module," Indian J. Sci. Technol., vol. 11, no. 26, pp. 1–5, Jul. 2018, doi: 10.17485/IJST/2018/V11I26/130559.

[30] B. Ait Skourt, A. El Hassani, and A. Majda, "Lung CT Image Segmentation Using Deep Neural Networks," Procedia Comput. Sci., vol. 127, pp. 109–113, Jan. 2018, doi: 10.1016/J.PROCS.2018.01.104.

[31] J. Zhang et al., "Viral Pneumonia Screening on Chest X-Rays Using Confidence-Aware Anomaly Detection," IEEE Trans. Med. Imaging, vol. 40, no. 3, pp. 879–890, Mar. 2021.

[32] M. M. Hasan, M. Md. Jahangir Kabir, M. R. Haque, and M. Ahmed, "A Combined Approach Using Image Processing and Deep Learning to Detect Pneumonia from Chest X-Ray Image," 3rd Int. Conf. Electr. Comput. Telecommun. Eng. ICECTE 2019, pp. 89–92, Dec. 2019, doi: 10.1109/ICECTE48615.2019.9303543.

[33] T. Samuel, D. Assefa, and O. Krejcar, "Framework for Effective Image Processing to Enhance Tuberculosis Diagnosis," Lect. Notes Comput. Sci. (including Subser. Lect. Notes Artif. Intell. Lect. Notes Bioinformatics), vol. 10752 LNAI, pp. 376–384, 2018, doi: 10.1007/978-3-319-75420-8_36.

[34] M. Norval, Z. Wang, and Y. Sun, "Pulmonary tuberculosis detection using deep learning convolutional neural networks," PervasiveHealth Pervasive Comput. Technol. Healthc., pp. 47–51, Dec. 2019, doi: 10.1145/3376067.3376068.

[35] E. Ayan and H. M. Ünver, "Diagnosis of pneumonia from chest X-ray images using deep learning," 2019 Sci. Meet. Electr. Biomed. Eng. Comput. Sci. EBBT 2019, Apr. 2019, doi: 10.1109/EBBT.2019.8741582.

[36] S. Bharati, P. Podder, and P. K. Paul, "Lung cancer recognition and prediction according to random forest ensemble and RUS Boost algorithm using LIDC data," Int. J. Hybrid Intell. Syst., vol. 15, no. 2, pp. 91–100, Jan. 2019, doi: 10.3233/HIS-190263.

[37] S. Perumal, S. Perumal, and T. Velmurugan, "Lung cancer detection and classification on CT scan images using enhanced artificial bee colony optimization," Int. J. Eng. Technol., vol. 7, no. 2.26, pp. 74–79, May 2018, doi: 10.14419/ijet.v7i2.26.12538.

[38] Garstka, J., & Strzelecki, M. (2020). Pneumonia detection in X-ray chest images based on convolutional neural networks and data augmentation methods. Signal Processing - Algorithms, Architectures, Arrangements, and Applications Conference Proceedings, SPA, 2020-September, 18–23. https://doi.org/10.23919/spa50552.2020.9241305

[39] Sharma, A., Raju, D., & Ranjan, S. (2018). Detection of pneumonia clouds in chest X-ray using image processing approach. 2017 Nirma University International Conference on Engineering, Nui CONE 2017, 2018-January, 1–4. https://doi.org/10.1109/NUICONE.2017.8325607

[40] Varshni, D., Thakral, K., Agarwal, L., Nijhawan, R., & Mittal, A. (2019). Pneumonia Detection Using CNN based Feature Extraction. Proceedings of 2019 3rd IEEE International Conference on Electrical, Computer and Communication Technologies, ICECCT 2019, 1–7. https://doi.org/10.1109/ICECCT.2019.8869364

[41] Tilve, A., Nayak, S., Vernekar, S., Turi, D., Shetgaonkar, P. R., & Aswale, S. (2020). Pneumonia Detection Using Deep Learning Approaches. International Conference on Emerging Trends in Information Technology and Engineering, Ic-ETITE 2020, 1–8. https://doi.org/10.1109/ic-ETITE47903.2020.152

[42] Rajasenbagam, T., Jeyanthi, S. & Pandian, J.A. (2021). Detection of pneumonia infection in lungs from chest X-ray images using deep convolutional neural network and content-based image retrieval

techniques. J Ambient Intell Human Comput, EBBT 2021. https://doi.org/10.1109/EBBT.2019.8741582

[43] Li, F., Engelmann, R., Pesce, L., Armato, S. G., & Mac Mahon, H. (2012). Improved detection of focal pneumonia by chest radiography with bone suppression imaging. European Radiology, 22(12), 2729–2735. https://doi.org/10.1007/s00330-012-2550-y

[44] Poornimadevi, C. S., & Helen Sulochana, C. (2016). Automatic detection of pulmonary tuberculosis using image processing techniques. Proceedings of the 2016 IEEE International Conference on Wireless Communications, Signal Processing and Networking, WiSP NET 2016, 798–802. https://doi.org/10.1109/WiSPNET.2016.7566243

[45] Panicker, R. O., Soman, B., Saini, G., & Rajan, J. (2016). A Review of Automatic Methods Based on Image Processing Techniques for Tuberculosis Detection from Microscopic Sputum Smear Images. Journal of Medical Systems, 40(1), 1–13. https://doi.org/10.1007/s10916-015-0388-y

[46] Liu, C., & Alcantara, M. F. (2016). TX-CNN : DETECTING TUBERCULOSIS IN CHEST X-RAY IMAGES USING CONVOLUTIONAL NEURAL NETWORK Partners in Health Per ´ u.

[47] Hooda, R., Sofat, S., Kaur, S., Mittal, A., & Meriaudeau, F. (2017). Deep-learning: A potential method for tuberculosis detection using chest radiography. Proceedings of the 2017 IEEE International Conference on Signal and Image Processing Applications, ICSIPA 2017, 497–502. https://doi.org/10.1109/ICSIPA.2017.8120663

[48] Saravanan, D., Bhavya, R., Archanaa, G. I., Karthika, D., & Subban, R. (2018). Research on Detection of Mycobacterium Tuberculosis from Microscopic Sputum Smear Images Using Image Segmentation. 2017 IEEE International Conference on Computational Intelligence and Computing Research, ICCIC 2017, 1–6. https://doi.org/10.1109/ICCIC.2017.8524222

[49] Shabut, A. M., Hoque Tania, M., Lwin, K. T., Evans, B. A., Yusof, N. A., Abu-Hassan, K. J., & Hossain, M. A. (2018). An intelligent mobile-enabled expert system for tuberculosis disease diagnosis in real time. Expert Systems with Applications, 114, 65–77. https://doi.org/10.1016/j.eswa.2018.07.014

[50] Bai Y, Xu J, Chen L, et al: Inflammatory response in lungs and extrapulmonary sites detected by [18 F] fluorodeoxyglucose PET/CT in convalescing COVID-19 patients tested negative for coronavirus. Eur J Nucl Med Mol Imaging: 1-12, 2021.

[51] Martinez RB, Ghesani M, Ghesani N, et al: Asymptomatic SARS-CoV-2 infection-Incidental findings on FDG PET/CT. J Med Imaging Radiat Sci 2021.

[52] Jacobi A, Chung M, Bernheim A, Eber C: Portable chest X-ray in coronavirus disease-19 (COVID-19): A pictorial review. Clin Imaging 2020.

[53] Kim JY, Yoo J-W, Oh M, et al: 18F-fluoro-2-deoxy-D-glucose positron emission tomography/computed tomography findings are different between invasive and non invasive pulmonary aspergillosis. J Comput Assist Tomogr 37:596-601, 2013.

[54] Qin C, Liu F, Yen T-C, Lan X: 18 F-FDG PET/CT findings of COVID19: A series of four highly suspected cases. Eur J Nucl Med Mol Imaging: 1-6, 2020.

[55] Zou S, Zhu X: FDG PET/CT of COVID-19. Radiology 296:E118, 2020 17. Dietz M, Chironi G, Claessens Y-E, et al: COVID-19 pneumonia: Relationship between inflammation assessed by whole-body FDG PET/CT and short-term clinical outcome. Eur J Nucl Med Mol Imaging 48:260- 268, 2021.

[56] Cristina Gamila Wakfie-Corieh et al. , Incidental findings suggestive of COVID-19 pneumonia in oncological patients undergoing 18F-FDG PET/CT studies: association between metabolic and structural lung changes. Journal of Nuclear Medicine Jun, 2021, jnumed.121.261915; DOI: 10.2967/jnumed.121.261915

[57] Randy Yeh, Ahmed Elsakka, Rick Wray, Rocio Perez Johnston, Natalie C. Gangai, Hooman Yarmohammadi, Heiko Schoder, Neeta Pandit-Taskar, "FDG PET/CT imaging features and clinical utility in COVID-19", Clinical Imaging, Volume 80, 2021, Pages 262-267, ISSN 0899-7071, https://doi.org/10.1016/j.clinimag.2021.08.002.

[58] Setti, L., Bonacina, M., Meroni, R. et al. Increased incidence of interstitial pneumonia detected on [18F]-FDG-PET/CT in asymptomatic cancer patients during COVID-19 pandemic in Lombardy: a casualty or COVID-19 infection?. Eur J Nucl Med Mol Imaging 48, 777–785 (2021). https://doi.org/10.1007/s00259-020-05027-y

[59] Fu, C., Zhang, W., Li, H. et al. FDG PET/CT evaluation of a patient recovering from COVID-19. Eur J Nucl Med Mol Imaging 47, 2703–2705 (2020). https://doi.org/10.1007/s00259-020-04958-w

[60] Bahloul, A., Boursier, C., Jeulin, H. et al. CT abnormalities evocative of lung infection are associated with lower 18F-FDG uptake in confirmed COVID-19 patients. Eur J Nucl Med Mol Imaging 48, 282–286 (2021). https://doi.org/10.1007/s00259-020-04999-1